

Size Distribution of Barrel-Stave Aggregates of Membrane Peptides: Influence of the Bilayer Lateral Pressure Profile

Robert S. Cantor

Department of Chemistry, Dartmouth College, Hanover, New Hampshire 03755 USA

ABSTRACT Some membrane peptides, such as Alamethicin, form barrel-stave aggregates with a broad probability distribution of size (number of peptides in the aggregate). This distribution has been shown to depend on the characteristics of the lipid bilayer. A mechanism for this influence is suggested, in analogy to earlier work on the effects of changes in bilayer composition on conformational equilibria in membrane proteins, that is based on coupling of shifts in the distribution of lateral pressures in the bilayer to depth-dependent changes in the lateral excluded area that accompanies the formation of an aggregate. Thermodynamic analysis is coupled with a simple geometric model of aggregates of kinked cylindrical peptides and with results of previously calculated lateral pressure distributions to predict the effects of changes in bilayer characteristics on aggregate size distributions, in qualitative agreement with experimental results.

INTRODUCTION

Alamethicin (Alm) is a well-studied example of a peptide that inserts and aggregates within cell membranes to form conducting channels (Sansom, 1993; Cafiso, 1994). Conductivity measurements suggest a barrel-stave arrangement around an aqueous pore, with a broad distribution of aggregation number n , i.e., the number of peptides in the aggregate (Sansom, 1991; Keller et al., 1993). This probability distribution has been shown to depend on the characteristics of the bilayer lipids, in particular through changes in the strength of head-group repulsions (Keller et al., 1993; Bezrukov et al., 1998). The mechanism of this influence on aggregate size is not known. Theoretical analysis (Dan and Safran, 1998) suggests that it may arise from a distortion of the bilayer around the aggregate, that results from a coupling of the noncylindrical shape of the aggregate with the curvature elastic properties (monolayer spontaneous curvature and curvature elastic modulus) of the lipid bilayer. It has also been suggested (Lewis and Cafiso, 1999; Bezrukov, 2000) that differences in bilayer thickness create a varying degree of hydrophobic mismatch that could cause a significant shift in the aggregate probability distribution. In the present work, another possible mechanism is suggested that arises from the effect of the lateral stress distribution on the equilibrium among different aggregates, and that is independent of any perturbation of the lipid bilayer in the vicinity of the aggregate.

This putative mechanism is analogous to that proposed to understand the influence of changes in bilayer composition on the conformational equilibria of intrinsic membrane proteins (Cantor, 1997, 1999a,b, 2001). The lipid bilayer of a cell membrane is characterized by a distribution of lateral

pressure densities $p(z)$ that varies strongly with depth in the bilayer z . Large positive lateral pressures within the hydrocarbon core (arising from reduced chain conformational entropy) and head-group electrostatic repulsions are balanced by negative lateral pressures (tensions) largely localized to the aqueous interfacial regions (Israelachvili et al., 1980; Seddon, 1990; Xiang and Anderson, 1994; Ben-Shaul, 1995; Seddon and Templer, 1995; Cantor, 1997, 1999a,b; Harris and Ben-Shaul, 1997; Venturoli and Smit, 1999; Lindahl and Edholm, 2000). Variations in the molecular characteristics of the lipids, such as the length or degree of unsaturation of the acyl chains, the strength of head-group repulsions, or the incorporation of cholesterol or other amphiphilic solutes causes a redistribution of the lateral stresses within the bilayer (Cantor, 1999a, 2001). Inclusions within the membrane, such as peptides or aggregates of peptides, are subjected to these lateral pressures. As is true for conformational transitions of intrinsic membrane proteins, the formation of an aggregate (either from smaller aggregates or from monomers) is accompanied by a change in the cross-sectional area $\Delta A(z)$, that varies with depth in the bilayer z . The resulting depth-dependent lateral expansion or contraction of the bilayer is characterized by a quantity of mechanical work that depends both on $p(z)$ and $\Delta A(z)$. Because $\Delta A(z)$ depends on the size of the aggregate, as will be discussed below for a simple geometric model, a redistribution of pressures resulting from a change in bilayer composition can cause a significant shift in the probability distribution of peptide aggregates.

The remainder of this paper is presented in three sections. First, simple thermodynamic arguments are used to obtain relationships among the equilibrium concentrations of aggregates of different n as a function of the area change of aggregation and of changes in the pressure profile for different lipid bilayers. Then, a simple geometric model is developed for kinked cylindrical peptides that provides an explicit form for the n -dependence of ΔA , which permits the general expressions for the aggregate concentrations to be

Submitted November 12, 2001, and accepted January 29, 2002.

Address reprint requests to Robert S. Cantor, Dept. of Chemistry, Dartmouth College, Hanover, NH 03755. Tel.: 603-646-2504; Fax: 603-646-3946; E-mail: rcantor@dartmouth.edu.

© 2002 by the Biophysical Society

0006-3495/02/05/2520/06 \$2.00

rewritten in a particularly simple form that depends only on changes in the first and second integral moments of the lateral pressure profiles. Shifts in the probability distributions accompanying changes in bilayer composition are then determined using results of statistical mechanical calculations from previous work (Cantor, 1999a), and are compared to experimental results.

THERMODYNAMIC RELATIONSHIPS

The relationships among the equilibrium concentrations of peptide monomers and aggregates of varying n are determined by setting $\mu_1 = \mu_2 = \mu_3 = \dots$ where μ_n represents the chemical potential of the peptide in an n -mer, i.e., an aggregate comprising n peptides. Let μ_n° represent the value in its "standard state", i.e., at unit concentration of n -mers and in a bilayer of standard composition characterized by a lateral pressure profile $p_0(z)$. Define $z = 0$ at the center of the bilayer of thickness $2h$, which thus extends from $z = -h$ to $z = h$. The peptide chemical potential in the aggregate subject to a different pressure profile $p(z)$ is then (Cantor, 1997)

$$\mu_n = \mu_n^\circ + (k_B T/n) \ln c_n + \int_{-h}^h \Delta p(z) A_n(z)/n \, dz, \quad (1)$$

where c_n represents the bilayer concentration of n -mer aggregates, $\Delta p(z) = p(z) - p_0(z)$, and $A_n(z)$ represents the depth-dependent cross-sectional area of the aggregate. The prefactor of $1/n$ in the logarithmic term accounts for the reduction in the translational entropy due to aggregation (Israelachvili et al., 1980). Using Eq. 1, the equilibrium condition $\mu_1 = \mu_n$ can be reexpressed as

$$n(\mu_1^\circ - \mu_n^\circ)/k_B T = \ln(c_n/c_1^n) + \alpha_n, \quad (2)$$

where

$$\alpha_n = (k_B T)^{-1} \int_{-h}^h \Delta p(z) \Delta A_n(z) \, dz. \quad (3)$$

In the above expressions, c_1 represents the bilayer concentration of peptide monomers, and $\Delta A_n = A_n - nA_1$ is the depth-dependent area change of formation of an n -mer from monomers. This general expression (for arbitrary pressure profile) must be valid for the bilayer of standard composition, for which $\Delta p(z) = 0$, and thus

$$n(\mu_1^\circ - \mu_n^\circ)/k_B T = \ln(c_{n,0}/c_{1,0}^n), \quad (4)$$

where $c_{n,0}$ and $c_{1,0}$ represent, respectively, the equilibrium bilayer concentrations of n -mers and monomers in a bilayer of standard pressure profile $p_0(z)$. From Eqs. 2 and 4, the standard chemical potentials can be eliminated to give an

expression for the effect of the change in pressure profile on the equilibrium concentrations,

$$c_n/c_1^n = \exp(-\alpha_n) c_{n,0}/c_{1,0}^n \quad (5)$$

Because the lipid bilayer is self-assembled, the total lateral pressure π acting upon it must be zero, and thus $\pi = \int p(z) \, dz = 0$. Any shift in the pressure distribution $\Delta p(z)$ must occur without a change in the total lateral pressure; increased pressure at certain depths in the bilayer must be accompanied by compensating decreases elsewhere, such that $\int \Delta p(z) \, dz = 0$. Thus the additive contributions to ΔA_n that are independent of z will not contribute to the integral in Eq. 3, regardless of $\Delta p(z)$.

Comparing Eq. 5 for two different aggregate sizes, n and m , gives

$$c_n/c_m = (c_1/c_{1,0})^{n-m} \exp(\alpha_m - \alpha_n) c_{n,0}/c_{m,0}. \quad (6)$$

This form will facilitate comparison of theoretical predictions with experimental results. In particular, if relative aggregate concentrations are compared at constant peptide monomer concentration in the bilayer, i.e., at $c_1 = c_{1,0}$, then Eq. 6 simplifies to

$$c_n/c_m = \exp(\alpha_m - \alpha_n) c_{n,0}/c_{m,0}. \quad (7)$$

Because the vast majority of peptide in the bilayer is in the monomer form, constant monomer concentration is essentially equivalent to constant total peptide bilayer concentration. However, the partitioning between the aqueous and bilayer environments may vary significantly with changes in bilayer composition, so, in general, this will not correspond to constant peptide concentration in the aqueous phase.

GEOMETRIC MODEL OF AGGREGATES

How does α_n depend on n ? A simple geometric model provides a first approximation. For purposes of describing the spatial distribution of excluded volume of the peptide, Alm peptides can be approximated as kinked cylinders, with the convex angle on the hydrophilic side of the peptide, as depicted in Fig. 1. The peptides are presumed to aggregate symmetrically around an open core, forming an hour-glass shape. Because the peptides are modeled as bent rods, they are close packed only at the depth in the bilayer, z^* , at which the kinks are localized. In this model, at a depth z in the plane (x - y) of the bilayer, the centers of the peptides form a regular polygon of n vertices, of area A_{poly} that varies with depth, being smallest at z^* . If R is the radial distance from the center of the aqueous pore to the center of a peptide, then

$$A_{\text{poly}} = nR^2/2 \sin(2\pi/n). \quad (8)$$

As shown in Fig. 1 A, θ_+ and θ_- are defined as the pair of angles formed by the peptide axis and the bilayer normal,

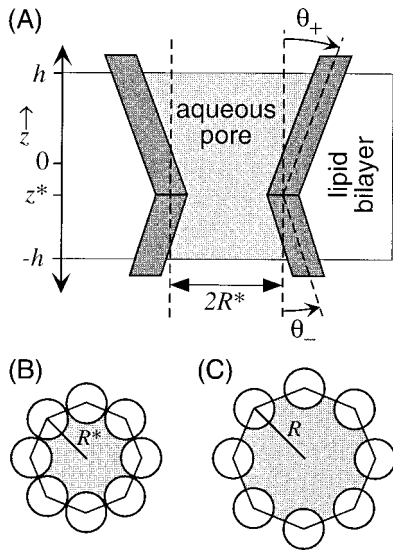


FIGURE 1 Simple geometric model of a peptide aggregate in a bilayer. Peptides are kinked cylinders, disposed with cylindrical symmetry around an aqueous pore, with angles θ_+ and θ_- representing the orientation of the peptide axis with respect to the z axis (perpendicular to the bilayer plane), above and below the kink (at z^*), respectively. (A) Slice in the x - z plane showing two peptides on opposite sides of the aggregate. The distance R from the peptide axis to the pore axis is smallest at $R(z^*) = R^*$. (B) Cross-section of an $n = 8$ aggregate at depth z^* in the bilayer (x - y) plane, at which the peptides are in contact. The gray area represents $\Delta A_n(z^*)$. (C) Cross-section of aggregate in the x - y plane, at depth $z \neq z^*$; note that $\Delta A_n(z) > \Delta A_n(z^*)$.

respectively, above ($z > z^*$) and below ($z < z^*$) the kink. The total bend angle of the peptide is $\theta = \theta_+ + \theta_-$. The distance R is determined by the number of peptides in the bundle n and the peptide radius r , and varies with z . At depth z^* ,

$$R^* = R(z^*) = r \csc(\pi/n). \quad (9)$$

For $z \neq z^*$, the radial distance to the peptide axis increases as

$$R(z) = R^* + |z - z^*| \sin \theta_{\pm}, \quad (10)$$

where $\theta_{\pm} = \theta_+$ for $z > z^*$, and $\theta_{\pm} = \theta_-$ for $z < z^*$. The area change $\Delta A_n = A_n - nA_1$ (the difference in the shaded areas in Fig. 1, B and C) is calculated by subtracting from A_{poly} the fractional area of the peptides that lie within it, yielding

$$\begin{aligned} \Delta A_n = & (n/2)[r \csc(\pi/n) + |z - z^*| \sin \theta_{\pm}]^2 \sin(2\pi/n) \\ & - n\pi r^2 \left(\frac{1}{2} - 1/n\right). \end{aligned} \quad (11)$$

As discussed above, only those additive contributions to ΔA_n that depend on z will make nonzero contributions to α_n , which can thereby be expressed as a sum of only two terms,

$$\alpha_n = an \cos(\pi/n) + bn \sin(2\pi/n), \quad (12)$$

with the two dimensionless parameters defined as

$$\begin{aligned} a &= 2r (k_B T)^{-1} \int_{-h}^h \Delta p(z) |z - z^*| \sin \theta_{\pm} dz, \\ b &= (k_B T)^{-1} \int_{-h}^h \Delta p(z) |z - z^*|^2 \sin^2 \theta_{\pm} dz. \end{aligned} \quad (13)$$

For a given redistribution of lateral pressures, and given the geometric characteristics of the peptide aggregate in the bilayer (z^* , $\sin \theta_+$, $\sin \theta_-$) the values of a and b can be predicted. As a particularly simple example, consider the symmetric case where the kink point in the peptide lies at the center of the bilayer ($z^* = 0$), and the two bilayer leaflets have identical composition so that the pressure profile is symmetric around the bilayer midplane: $p(z) = p(-z)$. Then the expressions for a and b simplify to

$$\begin{aligned} a &= 2r(\sin \theta_+ + \sin \theta_-) \Delta P_1 / k_B T, \\ b &= (\sin^2 \theta_+ + \sin^2 \theta_-) \Delta P_2 / k_B T, \end{aligned} \quad (14)$$

where the first and second integral moments of the pressure profile over one leaflet of the bilayer are defined as $P_i = \int z^i p(z) dz$ for $i = 1$ and 2 , respectively, and thus,

$$\Delta P_i = \int_0^h z^i \Delta p(z) dz. \quad (15)$$

Note that, if the peptide kink angle $\theta = \theta_+ + \theta_-$ is not too large, then $\sin \theta \approx \sin \theta_+ + \sin \theta_-$, and the expression for a simplifies to

$$a \approx 2r \sin \theta \Delta P_1 / k_B T, \quad (16)$$

i.e., the value of a depends far more on the kink angle of the peptide than on its overall tilt with respect to the bilayer normal.

RESULTS AND DISCUSSION

Using lattice statistical thermodynamic calculations, pressure profiles have previously been estimated (Cantor, 1999a) for a range of different bilayer lipid characteristics and composition, such as the length and degree of unsaturation of acyl chains, the strength of head-group repulsions, and the addition of cholesterol and small cosurfactants. Values of the integral moments P_1 and P_2 calculated therefrom for bilayers composed of lipids with weak head-group repulsions, as expected for phosphatidylethanolamine (PE) head groups, have been reported in earlier work (Cantor, 1999b) and are reproduced in Table 1, along with the calculated values of P_1 and P_2 for bilayers with the much stronger repulsions that characterize phosphatidylcholine (PC) head groups. Experimental results have been reported

TABLE 1 Predicted first and second moments of the pressure profile, for bilayers of varying acyl chain composition, with either weak (PE) or strong (PC) head-group repulsions

Acyl Chains*	Cholesterol (mol%)	$P_1/k_B T$ (\AA^{-1})		$P_2/k_B T$	
		PE	PC	PE	PC
di-14:0		-1.74	-1.18	-29.4	-17.9
di-16:0		-1.84	-1.30	-34.1	-21.8
di-16:0	10	-2.18	-1.55	-42.1	-27.4
di-18:0		-1.93	-1.41	-38.7	-25.9
di-20:0		-2.01	-1.52	-43.2	-30.0
di-18:1 $_{\Delta 9}$		-1.57	-1.28	-27.9	-21.3
di-18:1 $_{\Delta 9}$	10	-1.72	-1.42	-31.4	-24.5
di-18:2 $_{\Delta 9,12}$		-1.55	-1.27	-26.6	-21.0
di-18:3 $_{\Delta 9,12,15}$		-1.51	-1.25	-26.1	-20.5
di-18:3 $_{\Delta 6,9,12}$		-1.32	-1.13	-20.9	-17.2
di-20:4 $_{\Delta 5,8,11,14}$		-1.31	-1.14	-21.7	-18.4
di-22:6 $_{\Delta 4,7,10,13,16,19}$		-1.30	-1.15	-22.5	-19.4
di-22:6 $_{\Delta 4,7,10,13,16,19}$	10	-1.34	-1.20	-23.6	-20.6
16:0, 18:1 $_{\Delta 9}$		-1.65	-1.28	-29.4	-21.2
16:0, 18:1 $_{\Delta 9}$	10	-1.84	-1.45	-34.1	-25.2
16:0, 22:6 $_{\Delta 4,7,10,13,16,19}$		-1.36	-1.14	-23.4	-18.9
16:0, 22:6 $_{\Delta 4,7,10,13,16,19}$	10	-1.43	-1.23	-25.0	-20.8

*Acyl chains are symbolized as $N:M_{\Delta a,b,\dots}$, where N is the acyl chain length, M is the number of *cis* double bonds, and a, b, \dots are the locations of the unsaturation. 14:0, myristoyl; 16:0, palmitoyl; 18:0, stearoyl; 20:0, eadloyl; 18:1 $_{\Delta 9}$, oleoyl; 18:2 $_{\Delta 9,12}$, linoleoyl; 18:3 $_{\Delta 9,12,15}$, α -linolenoyl; 18:3 $_{\Delta 6,9,12}$, γ -linolenoyl; 20:4 $_{\Delta 5,8,11,14}$, arachidonoyl; 22:6 $_{\Delta 4,7,10,13,16,19}$, docosahexaenoyl.

(Keller et al., 1993) for the phospholipids dioleoyl phosphatidylcholine (DOPC) and dioleoyl phosphatidylethanolamine (DOPE), allowing comparisons to be made to the theoretical predictions for these lipids. From Table 1, $\Delta P_1 = P_1(\text{DOPE}) - P_1(\text{DOPC}) \approx -0.3 \text{ \AA}^{-1} k_B T$, and $\Delta P_2 \approx -6.5 k_B T$. To obtain rough estimates of α_n , the definitions of a and b for the symmetric peptide geometry (Eq. 14) are used as an illustrative example, and the peptide radius is set at $r \approx 5 \text{ \AA}$. The bend angle θ for Alm is likely to be in the range 20–30°, but, because it may exhibit significant fluctuations (Biggin et al., 1997; Bak et al., 2001; Tieleman et al., 1999), predictions are reported for various values in this range. Setting $m = n - 1$ in Eq. 7 provides predictions of the ratios of the relative probabilities of adjacent conductance states for the two bilayers, $(c_n/c_{n-1})_{\text{DOPE}}/(c_n/c_{n-1})_{\text{DOPC}} = \exp(\alpha_{n-1} - \alpha_n)$, which are graphed in Fig. 2 for a range of representative values of the peptide kink angles. In all cases, this factor is largest for small n and decreases to an asymptotic value with increasing n . Given the approximations in the calculations of P_1 and P_2 , and in the very simple geometric model of the aggregate, these results should be treated only as qualitatively accurate estimates. Keller et al. (1993) examined the relative frequencies of adjacent Alm conductance levels corresponding to $n = 6, 7$, and 8, and found an increase by a factor of roughly 5–10 for DOPE bilayers compared to DOPC bilayers, in qualitative agreement with the theoretical predictions. How-

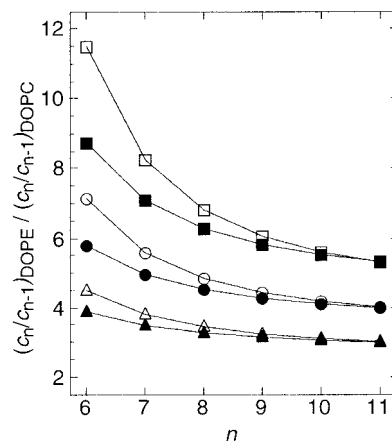


FIGURE 2 Predicted values of $(c_n/c_{n-1})_{\text{DOPE}}/(c_n/c_{n-1})_{\text{DOPC}} = \exp(\alpha_{n-1} - \alpha_n)$ as a function of the aggregation number n , at constant peptide monomer concentration in the bilayer. Results are given for a representative range of peptide kink angles and bilayer orientation. \square , $\theta = \theta_+ = 30^\circ, \theta_- = 0^\circ$; \blacksquare , $\theta = 30^\circ, \theta_+ = \theta_- = 15^\circ$; \circ , $\theta = \theta_+ = 25^\circ, \theta_- = 0^\circ$; \bullet , $\theta = 25^\circ, \theta_+ = \theta_- = 12.5^\circ$; \triangle , $\theta = \theta_+ = 20^\circ, \theta_- = 0^\circ$; \blacktriangle , $\theta = 20^\circ, \theta_+ = \theta_- = 10^\circ$. Lines are drawn as a guide to the eye.

ever, as mentioned above, this value can only be compared to the theoretical estimates at constant bilayer concentration of peptide monomer (essentially the total peptide concentration in the bilayer.) This is likely to be the case, at least approximately, for the aggregate distribution results of Keller et al. Although they find that the formation of aggregates in DOPE requires a 10-fold higher aqueous concentration of peptide than for DOPC under otherwise identical conditions, this is compensated by the difference in bilayer/aqueous partition coefficients for Alm, being 10-fold higher in DOPC than in DOPE (Lewis and Cafiso, 1999). Bezrukov et al. (1998) have also measured the change in c_n/c_{n-1} for lipids of the same acyl chain composition, as a function of the screening of electrostatic repulsions among charged head groups (by varying pH) and report an effect of similar magnitude. Opsahl and Webb (1994) measured changes in c_n/c_{n-1} in Alm aggregates resulting from a change in the total lateral pressure of the bilayer $\pi = \int p(z) dz$, at fixed bilayer composition. Unfortunately, it is not possible to compare the predictions of the present model to their experimental results, because the thermodynamic analysis developed here is only valid for $\pi = 0$, as discussed earlier.

As is evident from Table 1, the magnitude of the effect of altering the head-group repulsion strength, as discussed above for DOPC and DOPE, is predicted to depend on the acyl chains. For lipids with chains that are more highly unsaturated than oleate, the predicted effect of increasing head-group repulsions from phosphatidylethanolamine to phosphatidylcholine is considerably smaller in magnitude, whereas for those with saturated acyl chains, the calculated difference is considerably larger.

Using the data in Table 1, it is possible to predict the effect of other changes in lipid characteristics on c_n/c_{n-1} , for which experimental results have not yet been obtained. For example, increasing chain unsaturation causes a marked increase in both P_1 and P_2 , whereas increasing chain length has the opposite effect. Addition of cholesterol decreases P_1 and P_2 , the magnitude of the effect (for given cholesterol content) decreasing with increasing acyl chain unsaturation. Thus, the distribution of alamethicin aggregate size is expected to be skewed to the largest n for long saturated acyl chains, with increasing cholesterol content, and for weak head-group repulsions.

In the proposed mechanism, the first and second integral moments of the pressure distribution are key determinants of the aggregate probability distribution. These moments are also closely linked to the curvature elastic properties of the lipid monolayer leaflets (Helfrich, 1981; Szleifer et al., 1990; Seddon, 1990), which regulate the “nonlamellar” tendencies of lipids, i.e., the relative instability of the planar bilayer geometry with respect to formation of an inverted hexagonal phase. It is therefore not surprising that shifts in the aggregate probability distribution correlate well with this nonlamellar tendency (Keller et al., 1993; Dan and Safran, 1998; Lewis and Cafiso, 1999; Bezrukov, 2000).

It is useful to examine the characteristics of this geometrical model of kinked cylindrical peptides that might affect other contributions to aggregation (or insertion) equilibria. A potentially important example is the matching of the hydrophobic thickness of the peptide to that of the bilayer. In the present model, it has been assumed that both θ_+ and θ_- are independent of the number of peptides in the aggregate, i.e., the peptide kink angle and its tilt relative to the bilayer normal do not vary, and that the thickness of the bilayer is unaffected locally by the presence of the aggregate. Within these constraints, hydrophobic matching would not be expected to influence the distribution. However, if peptides in aggregates of varying sizes have different kink angle θ , or if they are oriented differently at fixed θ (e.g., a larger θ_+ with smaller θ_- to compensate), it could alter the peptide hydrophobic thickness, and thus the aggregate distribution. To estimate the magnitude of this effect, let the hydrophobic lengths of the two cylindrical parts of the peptide be ζ_+ and ζ_- . Their projections along the bilayer normal are approximately ($\zeta_+ \cos\theta_+$) and ($\zeta_- \cos\theta_-$), respectively, so the total hydrophobic thickness of the peptide along the bilayer normal is $\zeta \approx \zeta_+ \cos\theta_+ + \zeta_- \cos\theta_-$. The change in peptide hydrophobic thickness that accompanies a change in its orientation or kink angle is then

$$\Delta\zeta \approx \zeta_+ \Delta(\cos\theta_+) + \zeta_- \Delta(\cos\theta_-). \quad (17)$$

As a representative example, consider a peptide with $\zeta_+ = \zeta_- \approx 15 \text{ \AA}$, whose kink angle varies from 20° to 25° for different aggregates. For this case, the magnitude of $\Delta\zeta$ ranges from a minimum of 0.25 \AA for $\theta_+ = \theta_- = \theta/2$, up

to 0.5 \AA for $\theta_+ = \theta$, $\theta_- = 0^\circ$. As another example, consider a reorientation of this peptide at fixed kink angle $\theta = 20^\circ$, for which the change of largest possible magnitude would result for a tilt from $\{\theta_+ = 20^\circ, \theta_- = 0^\circ\}$ to $\{\theta_+ = \theta_- = 10^\circ\}$, for which case, $\Delta\zeta \approx 0.45 \text{ \AA}$. Clearly, even if peptides within barrel-stave aggregates of different sizes have significantly different orientation or kink angle, the shift in the size distribution mediated by changes in hydrophobic thickness is expected to be fairly small.

In summary, a mechanism has been proposed by which changes in lipid composition can modulate peptide aggregation equilibria. This mechanism is analogous to that used previously to describe the influence of changes in bilayer composition on conformational equilibria of membrane proteins. Both kinds of equilibria are characterized by a non-uniform change in lateral area that is accompanied by mechanical work, the quantity of which varies with the redistribution of bilayer lateral pressures that results from a change in bilayer composition. The predictions of this mechanism are found to be in qualitative agreement with existing experimental data on shifts in aggregate size distribution, but this certainly does not rule out other mechanisms, based on hydrophobic mismatch, perturbations of the surrounding lipid bilayer, etc. On the contrary, a wide range of mechanisms may well contribute to the influence of lipid properties on peptide and protein equilibria in membranes.

REFERENCES

- Bak, M., R. P. Bywater, M. Hohwy, J. K. Thomsen, K. Adlehorst, H. J. Jakobsen, O. W. Sørensen, and N. C. Nielsen. 2001. Conformation of alamethicin in oriented phospholipid bilayers determined by ^{15}N solid-state nuclear magnetic resonance. *Biophys. J.* 81:1684–1698.
- Ben-Shaul, A. 1995. Molecular theory of chain packing, elasticity and lipid–protein interaction in lipid bilayers. In *Structure and Dynamics of Membranes*. R. Lipowsky and E. Sackmann, editors. Elsevier/North Holland, Amsterdam, The Netherlands. 359–401.
- Bezrukov, S. M., R. P. Rand, I. Vodyanoy, and V. A. Parsegian. 1998. Lipid packing stress and polypeptide aggregation: alamethicin channel probed by proton titration of lipid charge. *Faraday Discuss.* 111: 173–183.
- Bezrukov, S. M. 2000. Functional consequences of lipid packing stress. *Curr. Opin. Coll. Int. Sci.* 5:237–243.
- Biggin, P. C., J. Breed, H. S. Son, and M. S. P. Sansom. 1997. Simulation studies of alamethicin–bilayer interactions. *Biophys. J.* 72:627–636.
- Cafiso, D. S. 1994. Alamethicin: a peptide model for voltage-gating and protein–membrane interactions. *Annu. Rev. Biophys. Biomol. Struct.* 23:141–165.
- Cantor, R. S. 1997. Lateral pressures in cell membranes: a mechanism for modulation of protein function. *J. Phys. Chem. B.* 101:1723–1725.
- Cantor, R. S. 1999a. Lipid composition and the lateral pressure profile in bilayers. *Biophys. J.* 76:2625–2639.
- Cantor, R. S. 1999b. The influence of membrane lateral pressures on simple geometric models of protein conformational equilibria. *Chem. Phys. Lipids.* 101:45–56.
- Cantor, R. S. 2001. Breaking the Meyer–Overton rule: predicted effects of varying stiffness and interfacial activity on the intrinsic potency of anesthetics. *Biophys. J.* 80:2284–2297.
- Dan, N., and S. A. Safran. 1998. Effect of lipid characteristics on the structure of transmembrane proteins. *Biophys. J.* 75:1410–1414.

- Harris, D., and A. Ben-Shaul. 1997. Conformational chain statistics in a model lipid bilayer: comparison between mean-field and Monte Carlo calculations. *J. Chem. Phys.* 106:1609–1619.
- Helfrich, W. 1981. Amphiphilic mesophases made of defects. In *Physics of Defects*. R. Balian, M. Kléman, and J.-P. Poirier, editors. North Holland, Amsterdam, The Netherlands. 716–755.
- Israelachvili, J., S. Marčelja, and R. Horn. 1980. Physical principles of membrane organization. *Q. Rev. Biophys.* 13:121–200.
- Keller, S. L., S. M. Bezrukov, S. M. Gruner, M. W. Tate, I. Vodyanoy, and V. A. Parsegian. 1993. Probability of alamethicin conductance states varies with nonlamellar tendency of bilayer phospholipids. *Biophys. J.* 65:23–27.
- Lewis, J. R., and D. S. Cafiso. 1999. Correlation between the free energy of a channel-forming voltage-gated peptide and the spontaneous curvature of bilayer lipids. *Biochemistry.* 38:5932–5938.
- Lindahl, E., and O. Edholm. 2000. Spatial and energetic-entropic decomposition of surface tension in lipid bilayers from molecular dynamics simulations. *J. Chem. Phys.* 113:3882–3893.
- Opsahl, L. R., and W. W. Webb. 1994. Transduction of membrane tension by the ion channel Alamethicin. *Biophys. J.* 66:71–74.
- Sansom, M. S. P. 1991. The biophysics of peptide models of ion channels. *Prog. Biophys. Mol. Biol.* 55:139–235.
- Sansom, M. S. P. 1993. Structure and function of channel-forming peptides. *Q. Rev. Biophys.* 26:365–421.
- Seddon, J. M. 1990. Structure of the inverted hexagonal (H_{II}) phase, and non-lamellar phase transitions of lipids. *Biochim. Biophys. Acta.* 1031:1–69.
- Seddon, J. M., and R. H. Templer. 1995. Polymorphism of lipid-water systems. In *Structure and Dynamics of Membranes*. R. Lipowsky and E. Sackmann, editors. Elsevier/North Holland, Amsterdam, The Netherlands. 97–160.
- Szleifer, I., D. Kramer, A. Ben-Shaul, W. M. Gelbart, and S. A. Safran. 1990. Molecular theory of curvature elasticity in surfactant films. *J. Chem. Phys.* 92:6800–6817.
- Tieleman, D. P., H. J. C. Berendsen, and M. S. P. Sansom. 1999. An alamethicin channel in a lipid bilayer: molecular dynamics simulations. *Biophys. J.* 76:1757–1769.
- Venturoli, M., and B. Smit. 1999. Simulating the self-assembly of model membranes. *Phys. Chem. Comm.* 10.
- Xiang, T.-X., and B. D. Anderson. 1994. Molecular distributions in interphases: statistical mechanical theory combined with molecular dynamics simulations of a model lipid bilayer. *Biophys. J.* 66:561–573.